Characterizing organic carbon dynamics during biostimulation of a uranium contaminated field site

M. A. Dangelmayr, L. A. Figueroa

Department of Civil and Environmental Engineering, Colorado School of Mines, 1500 Illinois St, Golden, CO 80401, USA e-mail: lfiguero@mines.edu

K. H. Williams

Earth Sciences Division, Lawrence Berkeley National Laboratory, Berkeley, CA 94720, USA

P. E. Long

Lawrence Berkeley National Laboratory, 1 Cyclotron Road, Berkeley, CA 94701, USA

Abstract

Uranium contamination of groundwater remains a pressing problem at many former uranium mining and milling operations, such as the Rifle, Integrated Field Research Challenge (IFRC) site. Biostimulation of the subsurface with an organic carbon source such as acetate, followed by the microbially-induced reductive precipitation of uranium has been proposed as an effective remediation strategy. While uranium bioreduction has been studied in several field experiments, the transformation and fate of injected carbon remains poorly understood. This study evaluated the impact of added organic carbon on the long-term biogeochemical attenuation of uranium in the subsurface of a former mill tailings site. Fluorescence and ultraviolet–visible absorbance analyses were used together with dissolved organic carbon (DOC) measurements to track organic carbon dynamics during and post-biostimulation of the 2011 Rifle IFRC experiment. An electron mass balance was performed on well CD01 to account for any unidentified carbon sinks. Measured DOC values increased to 1.76 mM-C during biostimulation, and to 3.18 mM-C post-biostimulation over background DOC values of 0.3–0.4 mM-C. Elevated DOC levels persisted for 90 days after acetate injections ceased. The electron mass balance revealed that assumed electron acceptors would not account for the total amount of acetate consumed. Excitation–emission matrices showed an increase in signals associated with soluble microbial products, during biostimulation, which disappeared post-biostimulation despite an increase in total DOC. Specific ultraviolet absorbance analyses, indicated that DOC present post-biostimulation is less aromatic in nature, compared to background DOC. Our results suggest that microbes convert injected acetate into a form of solid phase organic matter that may be available to sustain iron reduction post-stimulation.

Keywords

Soluble microbial products, Uranium, Bioremediation, Excitation–emission matrices, Groundwater, Dissolved organic carbon

Introduction

Contamination of groundwater by uranium remains a ubiquitous environmental challenge in all areas that are host to identified uranium resources (Mangini et al. 1997; Sheppard and Evenden 1988; USGS 2009). The microbial reduction and subsequent precipitation of the uranyl ion has been suggested as a possible remediation strategy (Anderson and Lovley 2002; Gorby and Lovley 1992) and been the subject of study at the Integrated Field Research Challenge (IFRC) sites at Rifle, CO for over a decade (Anderson et al. 2003; Williams et al 2013). Despite its promising applications, uranium bioreduction still faces several challenges that complicate long-term applications to the field. Sediment porosity can decrease during biostimulation as a consequence of microbial growth and mineral precipitation (Englert et al 2009; Li et al. 2009; Seifert and Engesgaard 2007, 2012). The resulting bioclogging of the aquifer may have diverted plumes away from remediation zones and monitoring wells. In addition, maintaining reducing conditions past active remediation remains difficult. During field studies at Rifle IFRC, CO, dissolved uranium concentrations returned to background values after the injection of the carbon source was terminated (Williams et al. 2011; Yabusaki et al. 2007). To make bioreduction a viable remediation tool for a variety of uranium contaminated sites, the long term stability and tendency for aquifer clogging need to be addressed.

The wastewater treatment literature has long recognized that microorganisms convert their primary organic substrate (e.g., acetate) into a range of solid-phase and soluble microbial products (SMP) (Barker and Stuckey 1999; Aquino and Stuckey 2008; Ni et al. 2009a; Wang et al. 2007; Ni et al. 2010a). The production and character of these microbially produced organic matter during bioreduction remains poorly understood. There has also been a significant lack of focus on closing the carbon and electron mass balances that have been shown to contain missing carbon sinks (Komlos et al. 2008; Regberg et al. 2011). The production of these organic compounds during biostimulation constitutes a possible carbon sink that could contribute to aquifer clogging as extracellular polymeric substances (EPS). More importantly, during periods of excess carbon availability bacteria have been shown to shuffle electrons into the production of storage polymers which may allow for continued microbial activity after injection of acetate is stopped (Krishna and Van Loosdrecht 1999; Freguia et al. 2007; Wang et al.

2007; Tian 2008). Studying the transformation pathways of organic substrates and the characteristics of microbially-produced organic matter in biostimulated systems can address some of the fundamental challenges that keep uranium bioremediation from being accepted by regulators and industry.

SMP comprise a complex mixture of organic compounds that include proteins, fulvic-like substances, biomass decay products, polysaccharides and extracellular polymeric substances (EPS) (Barker and Stuckey 1999; Aquino and Stuckey 2008) which may have varying degrees of bioavailability and chemical characteristics. For convenience, microbial process modeling frameworks group SMP into two operationally defined categories: Utilization associated products (UAP) and biomass associated products (BAP) (Laspidou and Rittman 2002). UAP are produced only during the growth stage in significant quantity and consist of organic compounds such as enzymes and sideraphores, metabolic intermediates or end products (Barker and Stuckey 1999). UAP can be a measurable carbon sink during active metabolism consuming between 5% and 20% of supplied substrate (Aquino and Stuckey 2004; Ni et al. 2009a). BAP are released through the degradation of biomass, which can include cell lysis products as well as the hydrolysis of microbially produced solid phase organic carbon such as EPS (Namkung and Rittmann 1986; Ni et al. 2010a). Naturally in the absence of substrate, BAP will dominate SMP composition. Since UAP and BAP stem from different microbial processes, they may serve as additional indicators to determine when and where microbes are actively growing. In addition, the bioavailability of dissolved organic carbon (DOC) might change when SMP composition shifts from UAP to BAP.

The complex composition of SMP has led to the use of spectroscopic bulk characterization to elucidate major features of soluble compounds in microbially active systems. Two spectroscopic bulk methods used to characterize SMP are 3-dimensional excitation–emission matrix fluorescence (EEM) and specific ultra-violet absorption at 254 nm wavelengths (SUVA) (Sheng and Yu 2006; Henderson et al. 2009; Ni et al. 2009b; Wang and Zhang 2010; Ni et al. 2010b). EEMs are three dimensional landscapes that plot a sample’s fluorescence intensity to the corresponding emission and excitation wavelength (Fellman et al. 2010; McKnight et al. 2001). Specific regions in those EEMs have been shown to correlate with either microbially produced organic matter or terrestrial organic matter (Chen et al. 2003; Sheng and Yu 2006; Wang et al. 2009). SUVA 254 nm values have been linked to a higher fraction of aromatic structures in DOC (Weishaar et al. 2003). A change in observed SUVA values could then indicate a shift in the bioavailability of SMP during or post-biostimulation (Marschner and Karsten

2003; Kang and Mitchell 2013). Spectroscopic techniques might offer new insights into the carbon dynamics of a biostimulated system both during active remediation and post-stimulation.

The purpose of this study was to determine, if in-situ biostimulation would produce SMP in measurable quantities and how long SMP production would persist once acetate addition was terminated. In addition, an attempt was made to close the carbon and electron mass balance for the biostimulated system to determine possible carbon sinks that are not accounted for solely by biomass growth and substrate utilization. Dissolved organic carbon and acetate were measured to estimate the amount of SMP. A conceptual model was used to divide SMP into two pools based on the postulated origin: UAP and BAP. Bulk analyses were used to characterize SMP by spectroscopic properties. Fluorescence spectroscopy was used to differentiate between UAP and BAP based on EEMs characteristics while SUVA was used to assess aromaticity and hence bioavailability of SMP compared to background DOC. We postulate that SMP maintain reducing conditions post-stimulation, by providing a continued supply of bioavailable carbon after acetate injections ceased, and that fluorescence spectroscopy can be used as an indicator of active microbial growth due to the presence of microbial signatures associated with UAP production. In addition, the carbon mass balance shows electron sinks unaccounted for by microbial biomass production or dissolved organic carbon alone, which could be indicative of the formation of a solid phase carbon sink, such as storage polymers.

Methods

Site description and field experiment

The Rifle, IFRC site was home to a uranium and vanadium mill whose tailings leached significant contamination into the groundwater. The site was cleaned up under Uranium Mine Tailing Reclamation Act (UMTRA) between 1992 and 1996 by removing the nearly 5 million tons of tailings. However, residual uranium (0.2–1.5 μM) present in the subsurface aquifer was not removed and the Rifle, IFRC site has been used to study uranium bioreduction extensively. The Rifle, IFRC site offered a unique opportunity to improve our understanding of the carbon cycle during and after biostimulation. In Fall 2011 the “Best Western” well gallery at the Rifle, IFRC site was used to examine organic carbon dynamics during bioremediation. The Rifle, IFRC site has been described in detail elsewhere (Anderson et al. 2003; Bao et al. 2014; Long 2012; Williams et al. 2011), while details of the well gallery, hydrogeology, and biostimulation experiments conducted a year prior to this research, are provided in Bao et al. (2014) and Long (2012). Briefly, the water table fluctuates seasonally at an average of 3.5 m below

surface based on the stage of the Colorado River. Figure 1 depicts the well gallery studied for the 2011 experiment. The gallery was aligned with the historic average groundwater flow direction at the site (0.1–0.6 m/d at a north-to-south orientation). Injection wells are denoted as CG, while observation and background wells have the CD and CU prefix, respectively. Wells were installed at a depth of ~6.5 m below surface. Acetate and bromide injection occurred over a 72-day period from 8/23/11 to 11/3/11. Injection solution contained 150 mM Sodium Acetate and 20 mM Sodium Bromide and was delivered at a flow rate to achieve groundwater concentrations of approximately 15 mM and 2 mM, respectively. Groundwater samples were collected before, during and after the 2011 acetate injection experiment.

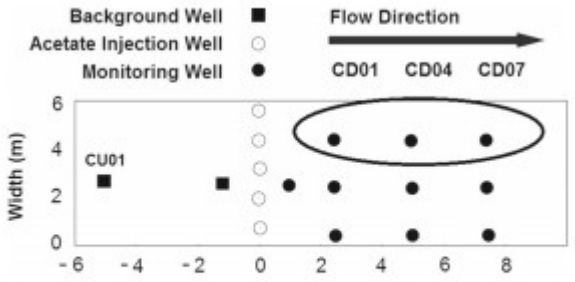

Fig. 1 Depiction of the portion of "Best Western" well gallery used for biostimulation with relevant observation wells CD01, CD04, CD07 and background well CU01 locations noted

Sample collection and preparation

Pumped groundwater samples (after ~ 12 L of purge volume) were taken from selected wells (CU01, CD01, CD04 and CD07). Samples for acetate, bromide, and groundwater chemical analysis were taken at least weekly over the 210 days of this investigation. Samples for anion and total inorganic carbon (TIC) analysis were filtered (PTFE; 0.45 µm) and stored in refrigerated, no-headspace HDPE and acid-washed glass vials, respectively, until analysis. Samples for organic carbon analysis were collected in brown 100 mL glass on a biweekly to monthly interval during biostimulation and a bimonthly interval post-stimulation. Samples were filtered in the laboratory with a 0.45 µm filter within 48 h after sampling and stored at 4 °C.

Groundwater chemical analysis

Acetate, bromide, and sulfate were measured using an ion chromatograph (ICS-2100, Dionex, CA) equipped with an AS18 column. TIC values (carbonates, bicarbonates, and dissolved carbon dioxide) were determined by sample acidification and sparging with the subsequent quantification of evolved CO_2 (TOC-VCSH, Shimadzu, Corp.) Samples for cation analysis

(including uranium) were filtered (PTFE; 0.45 μm) and acidified (0.2 mL 12 N HNO_3 per 20 mL sample), with concentrations determined using ion coupled plasma mass spectrometry (ICP-MS) (Elan DRCII ICP-MS, Perkin Elmer, Inc.) (USEPA 1994).

Organic acids, TOC, and SUVA analyses

An Aminex HPX-87H ion-exclusion column (Bio-Rad) with a UV/VIS detector (210 nm) was used to determine concentrations of organic acids (acetic, oxalic, citric, formic, succinic, and propionic acid) in collected samples. DOC concentrations were analyzed using a Shimadzu TOC-5000 analyzer with a high sensitivity catalyst. Total Fe of filtered samples was measured using a Perkin-Elmer Optima 3000 ICP-AES (EPA Method 6010B). Absorbance measurements were taken with a Perkin Elmer scanning UV–Vis Spectrophotometer for wavelength 254 nm in a 1 cm long cuvette. Specific UV absorbance (SUVA) values were calculated by dividing absorbance values by non-acetate DOC concentrations and the path length of the cuvette. Absorbance values were corrected for measured Fe concentrations using the method described in Weishaar et al. (2003).

Fluorescence analysis and EEM regional integration

Excitation–emission matrices (EEM) were obtained by scanning samples over an excitation (ex) range of 240–450 nm (10 nm intervals) and an emission (em) range of 280–550 nm (2 nm intervals) using a JY-Horiba/Spex Fluoromax-4 spectrofluorometer. A blank (MilliQ water) was scanned prior to each run and subtracted from each sample EEM to account for Raleigh scattering. The area under the Raman peak (ex 350 nm) of the same-day blank was used to normalize the intensities of all samples and a UV–Vis scan was used to apply an inner-filter correction to the EEMs. Since the same instrument was used for all fluorescence analyses, the EEMs used in this study are comparable to each other. Prior to fluorescence analysis, all samples were acidified to pH 3–3.3 and adjusted to room temperature 15 min prior to analysis to reduce the effect of ion quenching and increase fluorescence intensity (Chen et al. 2003; Ohno et al. 2008). The EEMs presented in this study were not diluted to a common DOC concentration, since intensities were non-detect whenever dilutions of higher than 2× were applied to samples taken after the stimulation period.

EEMs were divided into five characteristic fluorescence regions (Fig. 2) based on operationally defined excitation and emission boundaries by Chen et al. (2003). Regions I, II, and IV have been linked to protein-like compounds while regions III and V have been attributed to the presence of humic and fulvic acids. The cumulative fluorescence intensities for each region were calculated by integrating intensities within the defined boundaries in

MATLAB. Further details on the integration method can be found in Chen et al. (2003). Of specific interest to this study were changes in intensity of the biostimulation impacted wells relative to EEMs found in upgradient background well CU01. As a consequence, cumulative intensities in regions IV and V were normalized by dividing the average cumulative intensities measured in region IV and V in periodically collected background samples.

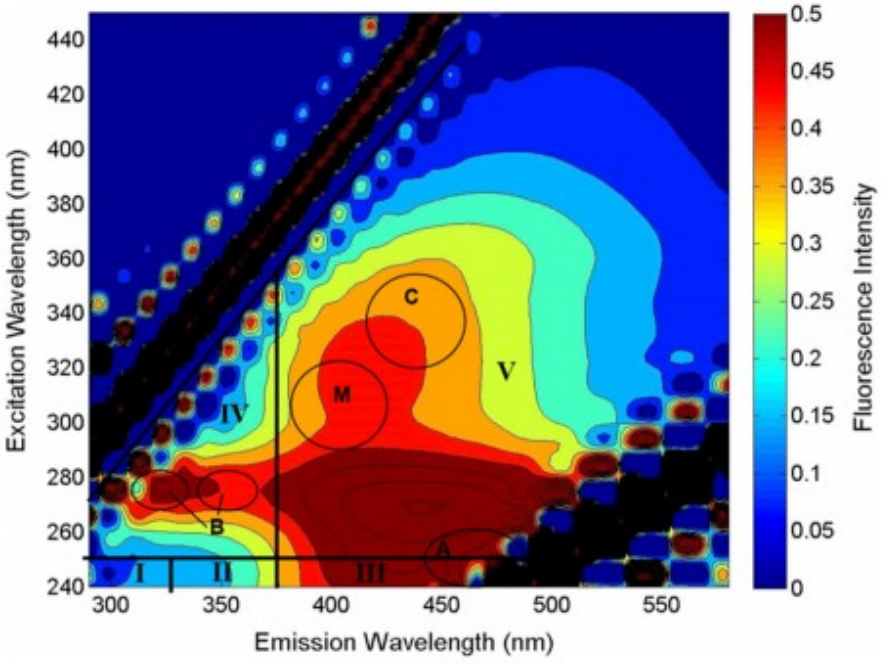

Fig. 2 A depiction of regions and common peaks in an EEM for well CD04. Regions I, II, IV and Peaks B are usually associated with organic matter of microbial origin. Regions III and V as well as Peaks C, M, and A indicate humic and fulvic like materials

Microbial stoichiometries and conceptual model

Relevant microbial reaction stoichiometries for iron, sulfate, and uranium reduction are presented below for acetate as the electron donor (Eqs. 1–3). The stoichiometries are based on the method presented in Rittman and McCarty (2001) using standard free energy corrected to pH 7 and an efficiency of 0.6 with the exception of iron reduction, which was based on an efficiency of 0.42 (Yabusaki et al. 2007).

$$\mathrm{FeOOH(s) + 1.9\ H^+ + 0.033\ NH_4^+ + 0.21\ CH_3COO^- \rightarrow Fe^{2+} + 0.033\ C_5H_7O_2N + 0.25\ HCO^- + 1.6\ H_2O} \quad (1)$$

$$\mathrm{SO_4^{2-} + 1.08\ CH_3COO^- + 0.052\ H^+ + 0.035\ NH_4^+ \rightarrow 0.035\ C_5H_7O_2N + 0.104\ H_2O + 2HCO_3^- + HS^-} \quad (2)$$

$$\mathrm{UO_2^{2+} + 0.067\ NH_4^+ + 0.42\ CH_3COO^- + 0.8\ H_2O \rightarrow UO_2(s) + 0.067\ C_5H_7O_2N + 0.5\ HCO_3^- + 2.15\ H^+} \quad (3)$$

The microbial stoichiometries were used to relate electron donor consumed to electron acceptor utilized, based on measured concentrations in the groundwater. The theoretical acetate utilization for each well could then be calculated through measured Fe(II), SO_4^{2-} and uranium concentrations and compared to actual acetate concentrations. Dissolved oxygen and nitrate reduction were not incorporated into the electron mass balance, since concentrations for both electron acceptors at the Rifle site have been repeatedly reported at micromolar to non-detect concentrations in background wells across several well galleries (Anderson et al. 2003; Williams et al. 2011; Long 2012; Bao et al. 2014).

SMP can be calculated by the difference between measured DOC and acetate concentrations if the result is significantly above background DOC observed in well CU01. A conceptual graph for the expected production of SMP during and after acetate injection is given in Fig. 3. The SMP components are based on a modeling framework proposed by Laspidou and Rittman (2002) where SMP is divided into two fractions based on origin. Utilization associated products (UAP) are produced as part of microbial growth. In a biostimulated system the relative fraction of UAP is expected to increase after a lag with acetate injection, plateau when acetate utilization reaches steady state, and decline to zero after acetate injection is terminated. Biomass associated products (BAP) stem from the degradation and solubilization of biomass. The fraction of BAP is expected to contribute to a small fraction of SMP during acetate injection but dominate post-stimulation as accumulated biomass and solid-phase organic carbon begins to degrade.

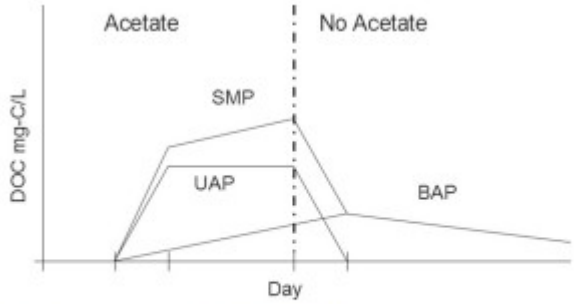

Fig. 3 A conceptual graph of SMP composition during the biostimulation event relating UAPs and BAPs to overall SMP production

Results

General performance

Biotransformations stimulated by acetate injection were assessed by analyzing acetate, bromide tracer, ferrous iron, organic carbon, uranium, and sulfate concentrations. Acetate, Fe(II), and sulfate are shown in Fig. 4, for observation wells CD01, CD04, and CD07. Uranium concentrations in observation wells and background wells are shown in Fig. 5 together with breakthrough curves of the bromide tracer for wells CD01, CD04, and CD07. Acetate and bromide concentration by day 120 were zero. Data for the inorganic indicators are presented from the day of initial acetate injection until 210 days after acetate injection was terminated. The production of ferrous iron and the removal of uranium relative to background concentrations are still evident at day 282 even though uranium begins to rebound after acetate injections are stopped.

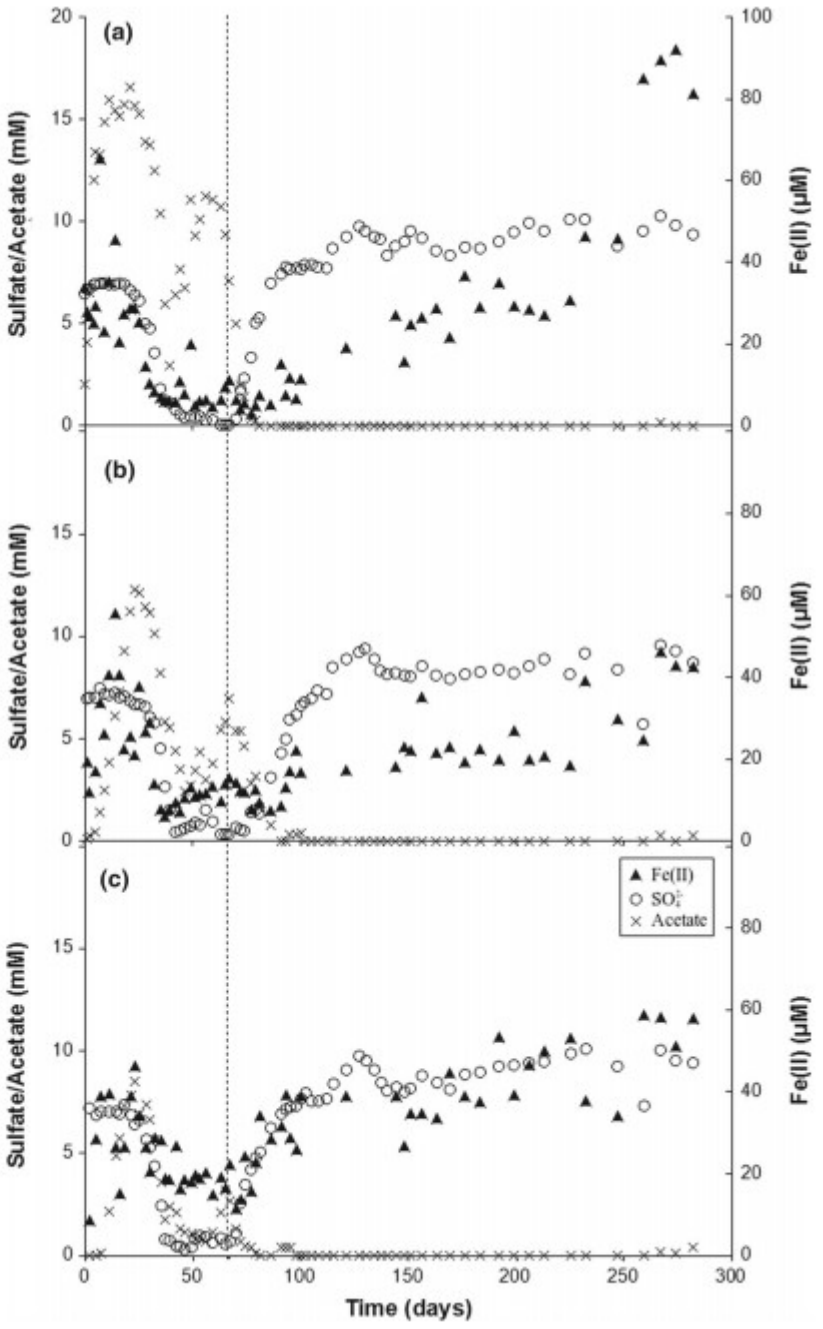

Fig. 4 Acetate (×), Fe(II) (▲) and SO_4^{2-} (○) concentrations for wells CD01 (**a**), CD04 (**b**), and CD07 (**c**). Acetate and sulfate concentrations are given in mM, while Fe(II) concentrations are in µM. The dotted line show the end of the stimulation period

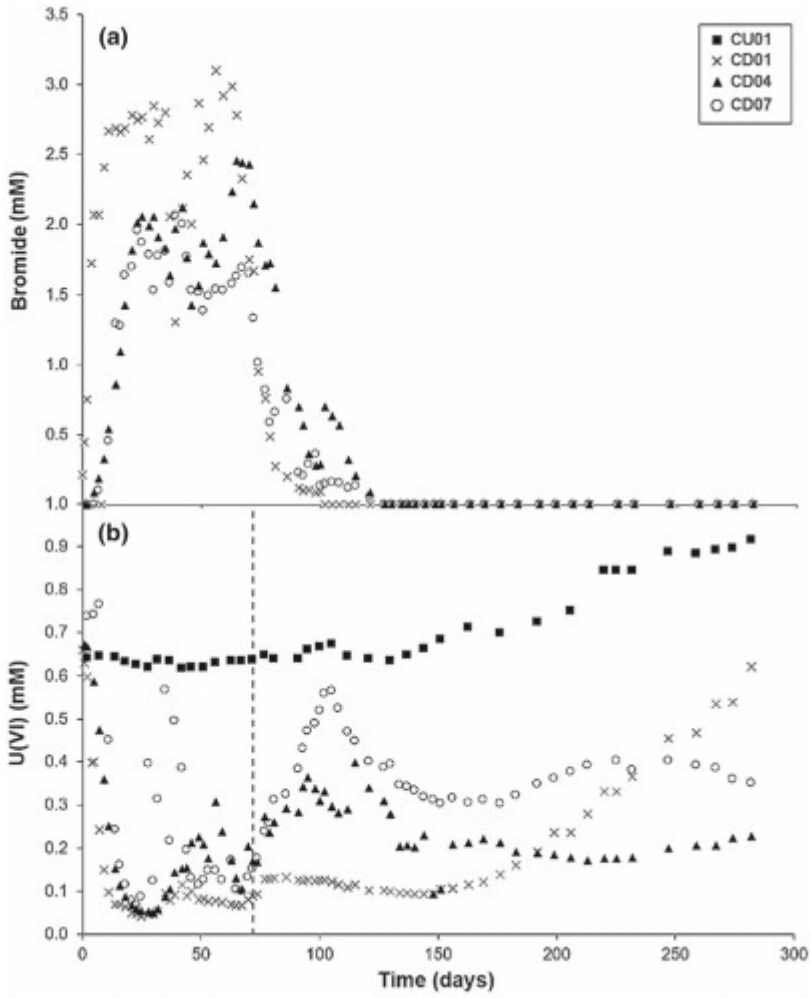

Fig. 5 Dissolved bromide (**a**) and uranium (**b**) concentration at wells CD01 (×), CD04 (▲) and CD07 (○) as well as background well CU01 (■) over the 282 days of the carbon cycling investigation. The dashed line at day 72 represents the end of active stimulation

Organic carbon analyses

Non-acetate DOC was calculated by subtracting measured acetate concentrations as mM-C from the measured DOC (mM-C) and is presented in Fig. 6. DOC concentrations in observation wells were compared to DOC from background well CU01. Any organic carbon above background values was considered to be of microbial origin (SMP) produced during biostimulation. Determining non-acetate DOC concentrations was difficult for CD01 during the first 28 days, as acetate concentrations ranged up to 15 mM-C. Small instrument errors in either DOC or acetate would have overshadowed actual non-acetate DOC. Most observation wells experienced elevated DOC values ranging from 0.67 mM-C up to 1.76 mM-C during biostimulation and reaching up to 3.18 mM-C 32 days after injections ceased in well CD07. DOC concentrations in background well CU01 remained between 0.3 and 0.4 mM-C throughout the experiment. Elevated DOC concentrations persisted 169 days into the experiment.

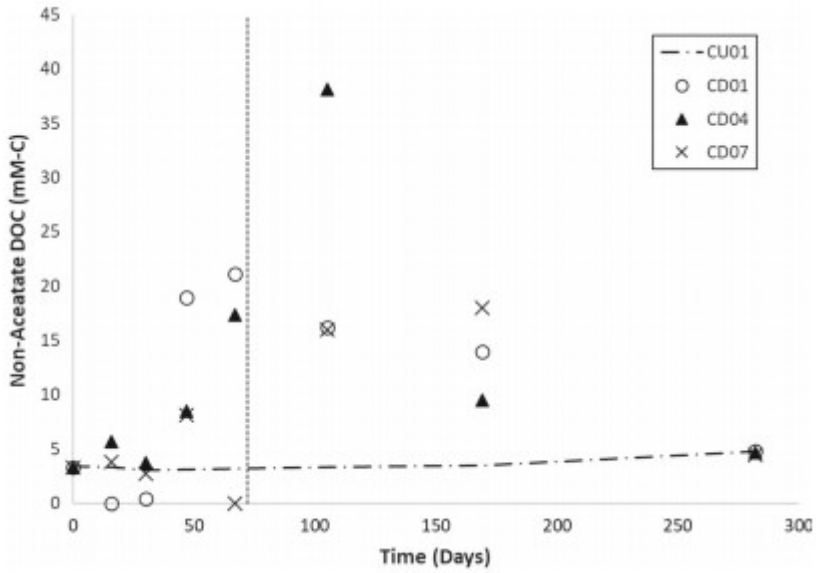

Fig. 6 Non-acetate carbon concentrations (as mM-C) for wells CD01 (×), CD04 (▲), CD07 (○), and background well CU01 (■, dashed line), from initial acetate injection through 210 days after injection ended. The dotted line at 72 days represents the end of the acetate injection period

Electron utilization accounting

Acetate utilization was analyzed for CD01 because of the difficulties in estimating hypothetical acetate influent past the 1st observation well. The injection ratio of 7.5:1 for acetate and bromide respectively, was used to estimate the expected acetate concentrations for well CD01. Electron equivalents of donor utilized, were based on 8 electron equivalents per mole of acetate. Utilization of electrons for the three important electron acceptors in the system was derived from stoichiometric Eqs. 1–3. Reduction of O_2 and NO_3^- was ignored due to low measured concentrations at the Rifle, IFRC site (2.0 µg/L and 1.4 µg-N/L respectively) (Bao et al. 2014). Sulfate utilization was calculated by subtracting measured SO_4^{2-} values from the average background value of 7.5 mM (± 0.093) from well CU01 from day 0 to day 72. Fe(III) utilization was calculated from the production of Fe(II). Uranium utilization was calculated by subtracting the measured uranium values from the average uranium concentrations in well CU01. Estimated total electrons utilized for iron and uranium reduction was less than 0.1 mM. Figure 7 shows the electrons utilized for sulfate reduction during acetate injection. On average, a daily 20.8 mM of electrons (or 5.2 mM-C) remained unaccounted for throughout the injection period for well CD01. Electron deficits ranged from 2.4 mM on day 4 to 38.7 mM on day 30. Between 0.31 mM and 4.1 mM carbon was unaccounted for during the first 20 days of stimulation, before sulfate reduction became observable.

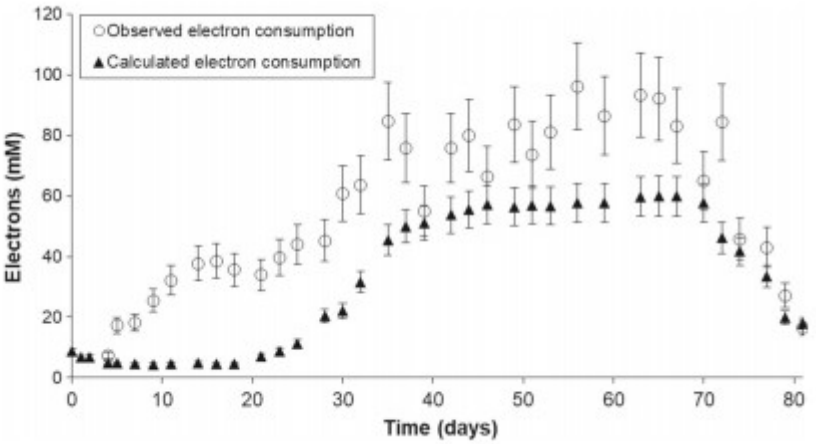

Fig. 7 Electrons available from consumed acetate (▲) and electrons utilized for sulfate, uranium, and iron reduction (○) versus time for well CD01. Assumed background SO_4^{2-} concentration of 7.5 mM, were calculated from the average SO_4^{2-} values for CU01 from day 0 to day 72. Error bars are based on the standard deviation in background sulfate concentrations and an assumed 10% error in the analytical techniques

SUVA 254 nm results

SUVA values in the background well CU01 ranged from 1.6 to 2.0 throughout the experiment. SUVA values for observation wells fluctuated during biostimulation from 0.64 to 2.98. The fluctuations are most likely due to difficulties in estimating accurate non-acetate DOC concentrations during the first 47 days due to the high acetate load. Post-stimulation values for observation wells on days 105 and 169, however, were relatively stable and hovered between 0.39 and 0.58.

Excitation–emission matrices and regional intensities

EEMs for the background well CU01 on day 16 and observation well CD04 on days 16, 67, and 282 are presented in Fig. 8. Well CD04 showed a well-defined fluorescence peak in the excitation emission (ex/em) characteristic of SMP (region IV) on day 67 when sulfate reduction dominated acetate consumption (Fig. 8c). Fluorescence intensity was already elevated in region IV, 16 days after the onset of biostimulation (Fig. 8b). During biostimulation EEMs of background well CU01 (Fig. 8a) did not show any significant deviations from each other in either the SMP region or the humic (region IV and V respectively). By day 105 or 33 days post-stimulation, the EEM for CD04 were indistinguishable from EEMs for background well CU01, with fluorescence intensity in region IV disappearing almost entirely. Similar trends were observed in wells CD01 and CD07, though not all EEMs exhibited characteristic peaks. Regional intensities for all observation wells, as a ratio of the average regional intensity of background well CU01, are shown in Figs. 9 (for region IV) and 10 (for region V). Fluorescence intensities for humic and fulvic peaks (characteristic for region V) increased during biostimulation and returned to background values post-stimulation in all three observation wells. At day 282 (or 210 days post-stimulation) a marked difference appeared in well CD07 (Fig. 11). Fluorescence peaks in region IV and II

increased to values 5× observed in the background well and showed characteristic peaks in the 350 nm emission range that were not observed even during biostimulation, even though DOC concentrations returned to background concentrations at day 282. In addition, signatures in region V (typically associated with humic and fulvic acids) disappeared. EEMs for wells CD01 or CD04 did not show any similar characteristics on day 282, and were almost identical to EEMs for background well CU01.

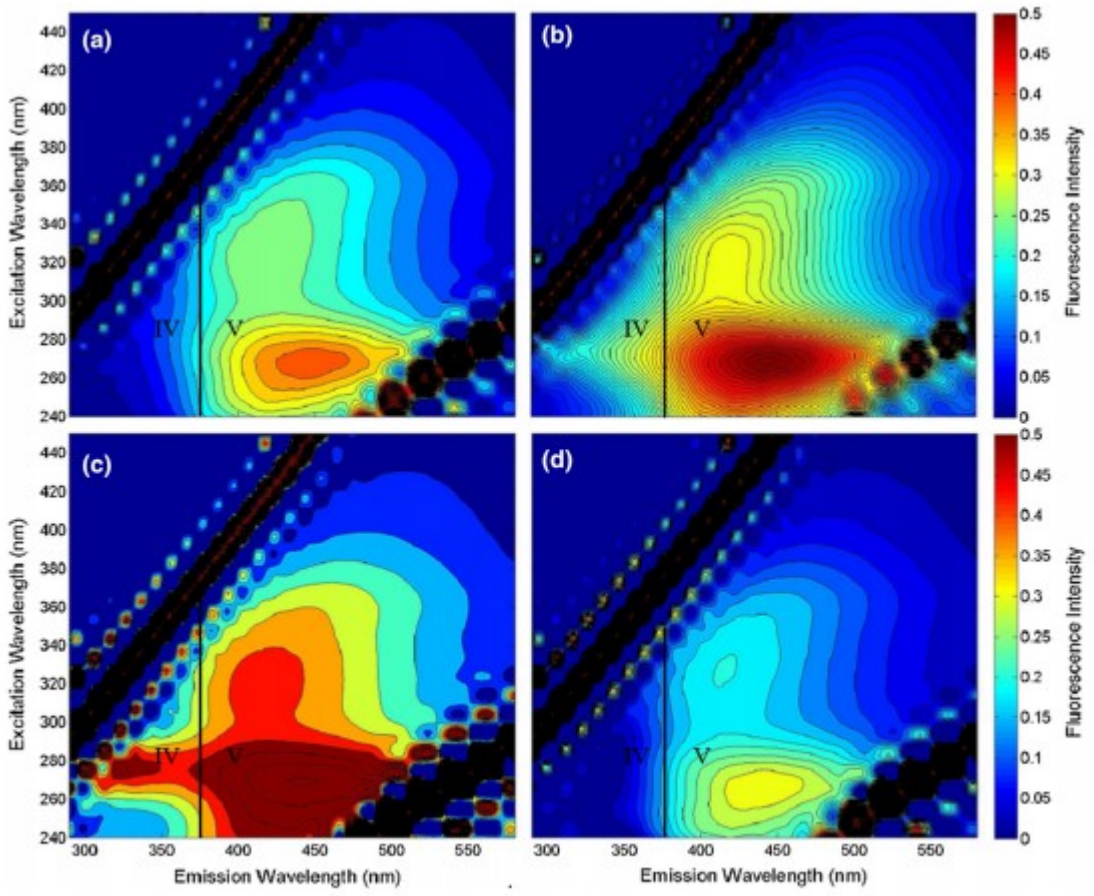

Fig. 8 EEMs for background (**a**) and well CD04, 16 days into biostimulation (**b**). EEM of observation well CD04 on day 67 (**c**) and day 105 (**d**)

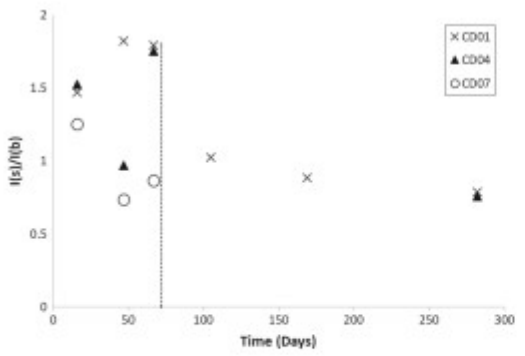

Fig. 9 Intensities of region IV in EEM samples from wells CD01 (■, blue), CD04 (◆, red), CD07 (●, green) as a ratio of the average intensity of EEMs from background well CU01 The dotted line at 72 days indicates the end of the stimulation period

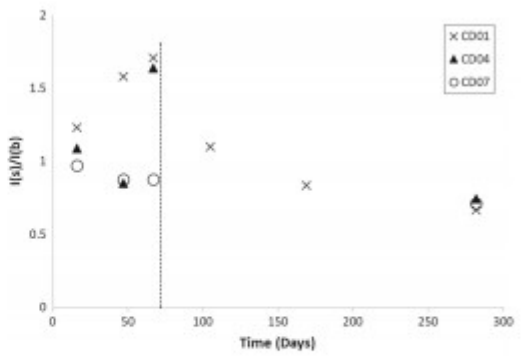

Fig. 10 Intensities of region V in EEM samples from wells CD01 (■, blue), CD04 (◆, red), CD07 (●, green) as a ratio of the average intensity of EEMs from background well CU01 The dotted line at 72 days indicates the end of the stimulation period

Fig. 11 EEM spectra for well CD07 at day 282

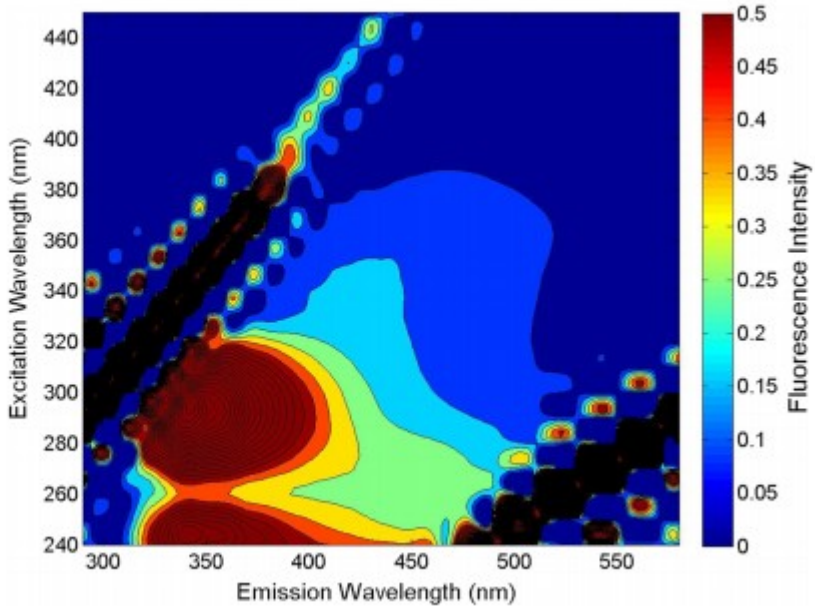

Discussion

The goal of the Rifle field experiments was to promote the reduction of uranium from the groundwater plume. Acetate was added above the estimated stoichiometric requirement for the microbial reduction of iron, uranium and sulfate. The highest amount of uranium was removed during acetate injection, however, measurable uranium reduction continued to occur 100 days after acetate injections were terminated (Fig. 5). Fe(II) measurements peaked at 64.2 µM in well CD01 7 days after the injection period started and remained elevated for the first 21 days at approximately 28 µM (Fig. 4). Meanwhile background Fe(II) values for well CU01 remained within a range of 0.9 to 13.6 µM during the entire observation period of 282 days. Sulfate reduction became noticeable after 28 days in well CD01. By

day 42 all wells experienced a 90% reduction in measured sulfate concentration. Iron reduction was difficult to assess during sulfate reduction because the formation of ferrous sulfide precipitates would have removed Fe(II) from solution. However, significant Fe(II) production was observed even after acetate injections were terminated. Fe(II) concentrations remained at approximately 20–40 μM in all wells after day 100 (28 days post-stimulation) and even surpassed Fe(II) concentration during biostimulation in well CD01 on day 259 (or 187 days post-stimulation). The persistence of uranium and iron reduction in the absence of added acetate, suggests that other forms of organic carbon were available to uranium and iron reducing bacteria post-stimulation.

The electron mass balance showed that the measured consumption of electron acceptors failed to account for a significant fraction of the acetate consumed in well CD01. During the initial iron reduction period (approximately day 7 to day 30) 88% (± 13%) of electrons donated from acetate were not utilized for microbial growth based solely on the stoichiometries in Eqs. 1–3. During sulfate reduction, (approximately days 44 to 72), an average of 33% of the consumed acetate still remained unaccounted for. These results hint that an unknown electron sink exists that was active within the first week of acetate injection (prior to sulfate reduction) and continued through the injection period. Other experimental systems studying uranium bioreduction also documented an incomplete carbon mass balance relative to the measured change in identified electron acceptors. Komlos et al. (2008) observed that only 1 to 1.5% of acetate was consumed by sulfate, iron, and uranium reduction. Regberg et al. (2011) could account for only 28% of acetate consumed by iron reduction in column experiments.

Methanogenesis has been suggested as a possible sink for acetate during biostimulation (Regberg et al. 2011; Komlos et al. 2008) and has been shown to occur concurrently with sulfate and iron reduction in saturated aquifer sediments (North et al. 2004; Gu et al. 2005b; Williams et al. 2011). However it is unlikely that methane production could explain the significant gap in the electron mass balance observed in this experiment. Methanogens and SRBs grow slowly compared to IRB (Capone and Kiene 1988; Gu et al. 2005b; Williams et al. 2011). Yet, a 33 mM electron gap in acetate utilization relative to terminal electron acceptors (TEAP) consumption occurred 16 days after biostimulation. In addition, an average 20.8 mM of electrons, or 2.6 mM acetate were unaccounted for during the biostimulation period. If methanogenesis was responsible for that loss, well CD01 would have produced roughly 2.4 mM of methane (or 52 mL CH_4 per liter of groundwater) each day. However the highest methane concentration measured in well

CD04 was only ~15 µM 20 days post-stimulation. The microbial reduction of manganese oxides (MnO_2) into soluble Mn(II) (Nealson and Myers 1992) is also thermodynamically favorable. However, Mn concentrations never exceeded 40 µM in any of the observation wells during the entire experimental period, which would contribute only a small fraction to the calculated electron consumption. Our results suggest that an unaccounted for carbon sink exists during biostimulation, assuming that iron and sulfate reduction represent the predominant metabolisms during the biostimulation experiment.

The wastewater treatment literature has long recognized that SMP production can constitute a significant carbon sink in microbial systems. Aquino and Stuckey (2003, 2004) reported as much as 37% of substrate being shuffled into SMP production under anaerobic conditions based on the presence of toxic metals or nitrogen availability. SMP have previously not been considered in the carbon cycle that affects the geochemistry of biostimulated aquifers even though organic carbon cycling is a primary driver of biogeochemical reactions that are harnessed to achieve bioremediation. During the Rifle IFRC biostimulation experiment, SMP concentrations more than doubled in wells CD04 and CD07, and increased five-fold for well CD01 on day 47 (Fig. 6), just as sulfate reduction become predominant (Fig. 4). It should be noted that the amount of SMP produced still fails to account for all the acetate consumed in well CD01. Roughly 1.6 and 1.8 mM-C of SMP were produced in well CD01 on days 47 and 67. However, the carbon mass balance suggests a carbon excess of over three times as much (~3.2 mM-C and 6.7 mM-C respectively) for the same days (Fig. 7).

SMP continued to be present in measurable concentrations even after acetate injections were halted on day 72. On day 105 (23 days after acetate injections), SMP concentrations ranged from 1.3 mM-C to 3.2 mM-C, while on day 169, measured SMP values remained between 0.79 mM-C and 1.5 mM-C among the three wells (Fig. 6). Microbes are known to shuffle carbon into storage polymers and EPS which may be released as substrate during starvation periods (Krishna and Van Loosdrecht 1999; Wang et al. 2007). In addition EPS are produced to grow biofilms to support adhesion to sediment particles. We postulate that the excess carbon consumption observed during the biostimulation period may have been shuffled into a solid organic matter phase and that the degradation of this solid-phase organic matter led to elevated DOC concentrations post-stimulation. Incidentally the peak SMP production in well CD07 on day 105 (Fig. 6) also coincided with a uranium spike observed during that same time period in well CD07 (Fig. 5). This post-stimulation release of uranium and DOC may be attributable to the re-

oxidation and/or complexation of uranium due to elevated organic matter (Ganesh et al. 1997; Artinger et al. 2002; Gu et al. 2005a), or the degradation of biomass that incorporated non-uraninite U(IV) (Bernier-Latmani et al. 2010).

It was hypothesized that the bulk characteristics of the SMP would be different during the stimulation and post-stimulation periods. Fluorescence and SUVA were used in this study to characterize SMP produced during the field experiment. Soluble SMP production was observable after 47 days, which coincided with the onset of sulfate reduction (as indicated by a drop in sulfate concentrations shown in Fig. 4). EEMs in Fig. 8 shows that a distinct protein-like signature started to appear in observation well CD04 on day 16 (Fig. 8b) while a characteristic protein-like peak can be observed on day 67 (Fig. 8c). After acetate injections were stopped, these protein-like peaks disappeared by day 105 (Fig. 8d). EEMs of background well CU01 (Fig. 8a) never displayed the protein-like peaks observed in the CD wells during the entire duration of the experiment. A similar trend was observed in well CD01 where fluorescence intensities in region IV (indicative of SMP production) experienced a significant spike over background intensities (Fig. 9) during the biostimulation period which dropped back to background intensities 33 days after the biostimulation period. Well CD07 also showed a mild increase in intensities in the SMP region (Fig. 9) on day 16, though the signature was less distinct and disappeared quickly on day 47. The absence of protein-like signatures can be explained by the acetate concentrations in well CD07, which dropped sharply on day 47 compared to well CD01 and CD04 (Fig. 4). A lack of substrate could have stymied microbial activity in well CD07 and as a consequence the UAP production correlating to the fluorescence intensity in region IV. The presence of these peaks are in agreement with other fluorescence literature and indicate SMP associated with microbial growth (or UAP) (Aquino and Stuckey 2008; Hur et al. 2009; Jarusutthirak and Amy 2007; Wang and Zhang 2010; Xie et al. 2010; Zhao et al. 2009).

On day 105 protein-like peaks were greatly diminished in all wells, and vanished completely on day 167 (Fig. 8d, Fig. 9). Overall fluorescence intensity in the SMP region was also greatly reduced after biostimulation ceased and dropped back to background values (Fig. 9). Initially all samples were diluted to a DOC concentration of ~4 ppm to prevent changes in peak appearance due to higher carbon content. However, fluorescence intensities vanished when dilutions were applied to samples collected after day 105. Undiluted, EEMs post-stimulation were essentially indistinguishable from samples in background wells, even though DOC concentrations were still elevated by a factor of 3 to 8 for all wells. The decrease of fluorescent

material in post stimulation EEMs would suggest that the produced SMP was composed of non-aromatic compounds found in EPS and polysaccharides.

We believe the SMP observed during acetate injection were most likely associated with UAP. This conjecture is based on the protein-like signatures in EEMs that have previously been linked to UAP formation. Xie et al. (2010) found that the protein-like peak at ex/em 280/350 nm increased in intensity during the growth phase of denitrifying bacteria in batch tests. This observation was consistent with UAP formation and an increase in the protein fraction of SMP. Meanwhile, Zhao et al. (2009) observed the release of protein-like fluorophores during the growth and stationary phase of *P. donghaiense*, while EEMs shifted to more humic and fulvic like components during the death phase. Overall EEMs could identify the production of UAP in bioremediation systems, through the presence of protein-like peaks during biostimulation. The produced SMP observed post-stimulation are therefore postulated to be BAP. In the absence of added substrate, microbial growth and corresponding UAP formation would be a limited and insignificant fraction of produced SMP (Aquino and Stuckey 2008). These results support our conceptual model illustrated in Fig. 3.

Fluorescence EEMs of samples from well CD07 210 days post-stimulation (Fig. 11) showed significant differences from EEMs of samples collected from either background wells or wells sampled during biostimulation.. A five-fold increase in intensity was observed in region IV (SMP), that surpassed values measured during active stimulation. In a literature review of fluorescence in wastewater treatment systems peaks in the < 380 nm emission regions have been correlated to increased BOD loading (Carstea et al. 2016) and indicate high microbial activity common to waste water and landfill leachates (He et al. 2011). The increased microbial activity stands in contrast to the actual DOC values which returned to background values of ~0.3 mM-C in all wells at day 282. However, a small but highly bioavailable amount of DOC would explain the continued production of Fe(II) observed in all three observation wells 210 days post-stimulation.

High SUVA values have been shown to correlate to increased aromaticity (Weishaar et al. 2003) in DOC and to be linked to more refractory DOC (Wang et al. 2009; Zhao et al. 2009). Batch tests on the microbial degradation of leaf litter demonstrated that the release of higher molecular weight compounds corresponded to a similar increase in SUVA (Hur et al. 2009). The higher molecular weight and high SUVA DOC was also determined to be more refractory based on rates of microbial utilization of DOC in these systems. In environmental systems, the effect of chemical structure on the bioavailability of soil organic matter remains ambiguous due to environmentally determined differences in solubilization rates (Lehmann

and Kleber 2015). However, in biostimulated systems, SUVA measurements could, nonetheless, serve as an indicator of shifts in the bioavailability of DOC, since any observed changes would be primarily caused by the production of SMP rather than the degradation of soil organic matter.

SUVA was difficult to quantify during the first 30 days of biostimulation. Acetate does not absorb UV light at 254 nm wavelengths, yet it was added at concentrations 50–100 times that of non-acetate DOC. Since instrumental errors for both the Schimadzu TOC analyzer and the HPLC were between 5% and 10%, calculated concentrations of non-acetate DOC were essentially within the margin of error for these instruments. In well CD04 non-acetate concentrations dipped to “zero” on day 67, most likely an artifact of these instrumental errors. SUVA values measured 100 days post-stimulation, dropped down to about a fourth of the observed background SUVA values, even though DOC concentrations were still elevated above background. Together with findings from previous literature (Hur et al. 2009; Wang et al. 2009) these data suggests that the reduction in SUVA values is mostly due to the addition of new microbially produced compounds such as solubilized EPS and storage polymers.

If a fraction of SMP was more bioavailable than the background DOC (as suggested by SUVA) then it could be available to prolong reducing conditions beyond the stimulation period. EEMs suggest that more complex SMP are produced during biostimulation while both EEMs and SUVA show that DOC is dominantly comprised of aliphatic, compounds (such as polysaccharides in EPS) up to 90 days post-stimulation. SMP measured on days 105 and 169 (33 and 97 days after acetate injections were stopped) contained excess electron equivalents (> 2 mM) to provide the stoichiometric donor requirement of the observed iron and uranium reduction (< 0.1 mM e- equivalents) (Fig. 6). By day 282, soluble SMP was below the resolution of the DOC measurements. However, the concentration of SMP needed to provide sufficient electron equivalents for the observed iron and uranium reduction was < 0.017 mM-C. These results suggest that the BAP portion of SMP could extend reducing conditions for at least 90 days and possibly longer post-biostimulation, by providing a more bioavailable carbon source than background DOC.

Our results indicate that a significant portion of carbon may have been shuffled into a carbon sink that cannot be related to the consumption of electron donors or UAP production, and may be indicative of the formation of microbial storage polymers and/or EPS. Elevated DOC levels that persisted 90 days post-stimulation were accompanied by continued Fe(II) production and uranium removal. Fluorescence EEMs showed intensities associated with microbial growth during biostimulation in all observation wells, while SUVA

analyses indicated that post-stimulation SMP were more bioavailable than background DOC. These results suggest that acetate was utilized to produce BAP during biostimulation, which became available after acetate injections ceased to sustain microbial activity. In addition, fluorescence spectroscopy and SUVA offer unique insights into the organic matter dynamics during biostimulation and inform understanding of microbial activity and the bioavailability of DOC during and post-stimulation.

Acknowledgements

We thank the NSF IGERT Program for partial funding of this research through a fellowship to M.A. Dangelmayr from the Colorado School of Mines SmartGeo Program (Project IGERT: Intelligent Geosystems; DGE-0801692). This project leveraged ongoing research at the Integrated Field Research Challenge Site at Rifle, CO, funded by the U.S. Department of Energy, Office of Science, Subsurface Biogeochemistry Research Program.

References

Anderson RT, Lovley DR (2002) Microbial redox interactions with uranium: an environmental perspective. Radioact Environ 2:205–223

Anderson RT, Vrionis HA, Ortiz-Bernad I, Resch CT, Long PE, Dayvault R, Peacock A (2003) Stimulating the in situ activity of *Geobacter* species to remove uranium from the groundwater of a uranium-contaminated aquifer. Appl Environ Microbiol 69(10):5884–5891

Aquino SF, Stuckey DC (2003) Production of soluble microbial products (SMP) in anaerobic chemostats under nutrient deficiency. J Environ Eng 129:1007–1014

Aquino SF, Stuckey DC (2004) Soluble microbial products formation in anaerobic chemostats in the presence of toxic compounds. Water Res 38:255–266

Aquino SF, Stuckey DC (2008) Integrated model of the production of soluble microbial products (SMP) and extracellular polymeric substances (EPS) in anaerobic chemostats during transient conditions. Biochem Eng J 38:138–146

Artinger R, Rabung T, Kim JI, Sachs S, Schmeide K, Heise KH, Bernhard G, Nitsche H (2002) Humic colloid borne migration of uranium in sand columns. J Contam Hydrol 58:1–12

Bao C, Wu H, Li L, Newcomer D, Long PE, Williams KH (2014) Uranium bioreduction rates across scales: biogeochemical hot moments and hot spots during a biostimulation experiment at Rifle, Colorado. Environ. Sci. Technol. 48:10116–10127

Barker DJ, Stuckey DC (1999) A review of soluble microbial products (SMP) in wastewater treatment systems. Water Res 33:3063–3082

Bernier-Latmani R, Veeramani H, Vecchia ED, Junier P, Lezama-Pacheco JS, Suvorova EI, Sharp JO, Wigginton NS, Bargar JB (2010) Non-uraninite products of microbial U (Vi) reduction. Environ Sci Technol 44:9456–9462

Capone DG, Kiene RP (1988) Comparison of microbial dynamics in marine and freshwater sediments: contrasts in anaerobic carbon catabolism. Limnol Oceanogr 33(4 Part 2):725–749. https://doi.org/10.4319/lo.1988.33.4part2.0725Google Scholar

Carstea EM, Bridgeman J, Baker A, Reynolds DM (2016) Fluorescence spectroscopy for wastewater monitoring: a review. Water Res 95:205–219

Chen W, Westerhoff P, Leenheer JA, Booksh K (2003) Fluorescence excitation–emission matrix regional integration to quantify spectra for dissolved organic matter. Environ Sci Technol 37:5701–5710

Englert A, Hubbard SS, Williams KH, Li L, Steefel CI (2009) Feedbacks between hydrological heterogeneity and bioremediation induced biogeochemical transformations. Environ Sci Technol 43:5197–5204

Fellman JB, Hood E, Spencer GM (2010) Fluorescence spectroscopy opens new windows into DOM dynamics in freshwater ecosystems: a review. Limnol Oceanogr 55:2452–2462

Freguia S, Rabaey K, Yuan Z, Keller J (2007) Electron and carbon balances in microbial fuel cells reveal temporary bacterial storage behavior during electricity generation. Environ Sci Technol 41:2915–2921

Ganesh R, Robinson KG, Reed GD, Sayler GS (1997) Reduction of hexavalent uranium from organic complexes by sulfate- and iron-reducing bacteria. Appl Environ Microbiol 63:4385–4391

Gorby YA, Lovley DR (1992) Enzymatic uranium precipitation. Environ Sci Technol 26:205–207

Gu B, Yan H, Zhou P, Watson DB (2005a) natural humics impact uranium bioreduction and oxidation. Environ Sci Technol 39:5268–5275

Gu B, Wu W, Ginder-Vogel MA, Yan H, Fields MW, Zhou J, Fendorf S, Criddle CS, Jardine PM (2005b) Bioreduction of uranium in a contaminated soil column. Environ Sci Technol 39:4841–4847

He X-S, Xi B-D, Wei Z-M, Jiang Y-H, Yang Y, An D, Liu H-L (2011) Fluorescence excitation–emission matrix spectroscopy with regional integration analysis for characterizing composition and transformation of dissolved organic

matter in landfill leachates. J Hazard Mater 190(1):293–299. https://doi.org/10.1016/j.jhazmat.2011.03.047

Henderson RK, Baker A, Murphy KR, Hambly A, Stuetz RM, Khan SJ (2009) Fluorescence as a potential monitoring tool for recycled water systems: a review. Water Res. 43:863–881

Hur J, Park MH, Schlautman MA (2009) Microbial transformation of dissolved leaf litter organic matter and its effects on selected organic matter operational descriptors. Environ Sci Technol 43:2315–2321

Jarusutthirak C, Amy G (2007) Understanding soluble microbial products (SMP) as a component of effluent organic matter (EfOM). Water Res 41:2787–2793

Kang P-G, Mitchell MJ (2013) Bioavailability and size-fraction of dissolved organic carbon, nitrogen, and sulfur at the Arbutus Lake watershed, Adirondack Mountains, NY. Biogeochemistry 115:213–234

Komlos J, Peacock A, Kukkadapu RK, Jaffé PR (2008) Long-term dynamics of uranium reduction/reoxidation under low sulfate conditions. Geochim Cosmochim Acta 72:3603–3615

Krishna C, Van Loosdrecht MC (1999) Effect of temperature on storage polymers and settleability of activated sludge. Water Res 33:2374–2382

Laspidou CS, Rittman BE (2002) A unified theory for extracellular polymeric substances, soluble microbial products, and active and inert biomass. Water Res 36:2711–2720

Lehmann J, Kleber M (2015) The contentious nature of soil organic matter. Nature 528:60. https://doi.org/10.1038/nature16069

Li L, Steefel CI, Williams KH, Wilkins MJ, Hubbard SS (2009) Mineral transformation and biomass accumulation associated with uranium bioremediation at Rifle, Colorado. Environ Sci Technol 43:5429–5435

Long PE (2012) Microbiological, geochemical and hydrologic processes controlling uranium mobility: an integrated field scale subsurface research challenge site at Rifle, Colorado, February 2011 to January 2012

Mangini A, Sonntag C, Bertsch G, Müller E (1997) Evidence for a higher natural uranium content in world rivers. Nature 278:337–339

Marschner B, Karsten K (2003) Controls of bioavailability and biodegradability of dissolved organic matter in soils. Geoderma 113:211–235

McKnight DM, Boyer EW, Westerhoff PK, Doran PT, Kulbe T, Andersen DT (2001) Spectrofluorometric characterization of dissolved organic matter for

indication of precursor organic material and aromaticity. Limnol Oceanogr 46:38–48

Namkung E, Rittmann BE (1986) Soluble microbial products (SMP) formation kinetics by biofilms. Water Res 20:795–806

Nealson KH, Myers CR (1992) Microbial reduction of manganese and iron: new approaches to carbon cycling. Appl Environ Microbiol 58(2):439–443

Ni BJ, Fang F, Xie WM, Sun M, Sheng GP, Li WH, Yu HQ (2009a) Characterization of extracellular polymeric substances produced by mixed microorganisms in activated sludge with gel-permeating chromatography, excitation–emission matrix fluorescence spectroscopy measurement and kinetic modeling. Water Res 43:1350–1359

Ni BJ, Fang F, Rittmann BE, Yu HQ (2009b) Modeling microbial products in activated sludge under feast–famine conditions. Environ Sci Technol 43:2489–2497

Ni BJ, Rittmann BE, Fang F, Xu J, Yu H (2010a) Long-term formation of microbial products in a sequencing batch reactor. Water Res 44:3787–3796

Ni B, Zeng RJ, Fang F, Xie W, Sheng G, Yu H (2010b) Fractionating soluble microbial products in the activated sludge process. Water Res 44:2292–2302

North NN, Dollhopf SL, Petrie L, Istok JD, Balkwill DL, Kostka JE (2004) Change in bacterial community structure during in situ biostimulation of subsurface sediment cocontaminated with uranium and nitrate. Appl Environ Microbiol 70:4911–4920

Ohno T, Amirbaham A, Bro R (2008) Parallel factor analysis of excitation–emission matrix fluorescence spectra of water soluble soil organic matter as basis for the determination of conditional metal binding parameters. Environ Sci Technol 42:186–192

Regberg A, Singha K, Tien M, Picardal F, Zheng Q, Schieber J, Roden E, Brantley S (2011) Electrical conductivity as an indicator of iron reduction rates in abiotic and biotic systems. Water Resour Res 47:W04509

Rittman BE, McCarty PL (2001) Environmental biotechnology: principles and applications. McGraw-Hill, New York

Seifert D, Engesgaard P (2007) Use of tracer tests to investigate changes in flow and transport properties due to bioclogging of porous media. J Contam Hydrol 93:58–71

Seifert D, Engesgaard P (2012) Sand box experiments with bioclogging of porous media: hydraulic conductivity reductions. J Contam Hydrol 136–137:1–9

Sheng GP, Yu HQ (2006) Characterization of extracellular polymeric substances of aerobic and anaerobic sludge using three-dimensional excitation and emission matrix fluorescence spectroscopy. Water Res 40:1233–1239

Sheppard SC, Evenden WG (1988) Critical compilation and review of plant/soil concentration ratios for uranium, thorium and lead. J Environ Radioact 8:255–285

Tian Y (2008) Behaviour of bacterial extracellular polymeric substances from activated sludge: a review. Int J Environ Pollut 32:78–89

USEPA (1994) U.S. EPA Method 200.8, Methods for the determination of the trace metals in waters and wastewaters. In: Methods for the determination of metals in environmental samples-supplement 1; EPA 600/R-94-111; U.S. Government Publishing Office, Washington DC, 1994

USGS (2009) Groundwater restoration at uranium in-situ recovery mines, South Texas Coastal Plain. No. 2009-1143

Wang ZP, Zhang T (2010) Characterization of soluble microbial products (SMP) under stressful conditions. Water Res 44:5499–5509

Wang ZW, Liu Y, Tay JH (2007) Biodegradability of extracellular polymeric substances produced by aerobic granules. Appl Microbiol Biotechnol 74:462–466

Wang Z, Wu Z, Tang S (2009) Characterization of dissolved organic matter in a submerged membrane bioreactor by using three-dimensional excitation and emission matrix fluorescence spectroscopy. Water Res 43:1533–1540

Weishaar JL, Aiken GR, Bergamaschi BA, Fram MS, Fujii R (2003) Evaluation of specific ultra-violet absorbance as an indicator of the chemical composition and reactivity of dissolved organic carbon. Environ Sci Technol 37:4702–4708

Williams KH, Long PE, Davis JA, Wilkins MJ, N’Guessan AL, Yang L, Newcomer D, Spane FA, Kerkhof LJ, McGuiness L, Dayvault R, Lovley DR (2011) Acetate availability and its influence on sustainable bioremediation of uranium-contaminated groundwater. Geomicrobiol J 28:519–539

Williams KH, Bargar JR, Lloyd JR, Lovley DR (2013) Bioremediation of uranium-contaminated groundwater: a systems approach to subsurface biogeochemistry. Curr Opin Biotechnol 24:489–497

Xie WM, Ni BJ, Zeng RJ, Sheng GP, Yu HQ, Song J, Le DZ, Bi XJ, Liu CQ, Yang M (2010) Formation of soluble microbial products by activated sludge under anoxic conditions. Appl Microbiol Biotechnol 87:373–382

Yabusaki SB, Fang Y, Long PE, Resch CT, Peacock AD, Komlos J, Jaffe PR, Morrison SJ, Dayvault RD, White DC, Anderson RT (2007) Uranium removal from groundwater via in situ biostimulation: field-scale modeling of transport and biological processes. J Contam Hydrol 93:216–235

Zhao W, Wang J, Chen M (2009) Three-dimensional fluorescence characteristics of dissolved organic matter produced by *Prorocentrum donghaiense* Lu. Chin J Oceanol Limnol 27:564–569